NASA Technical Memorandum 81424

EXPERIMENTS ON H_2-O_2 MHD POWER GENERATION

J. Marlin Smith
Lewis Research Center
Cleveland, Ohio

Prepared for the
Third World Hydrogen Energy Conference
Tokyo, Japan, June 23-26, 1980

EXPERIMENTS ON H_2-O_2 MHD POWER GENERATION

J. Marlin Smith

NASA Lewis Research Center
Cleveland, OH 44135

ABSTRACT

MHD power generation experiments utilizing a cesium-seeded H_2-O_2 working fluid have been carried out using a diverging area Hall duct having an entrance Mach number of 2. The experiments are conducted in a high-field strength cryomagnet facility at field strengths up to 5 tesla. The effects of power takeoff location, axial duct location within the magnetic field, generator loading, B-field strength, and electrode breakdown voltage were investigated. For the operating conditions of these experiments it is found that the power output increases with the square of the B-field and can be limited by choking of the channel or interelectrode voltage breakdown which occurs at Hall fields greater than 50 volts/insulator. Peak power densities of greater than 100 MW/M^3 have been achieved.

KEYWORDS

Magnetohydrodynamics; power generation; H_2-O_2 combustion; hydrogen economy; cryomagnet

I. INTRODUCTION

The utilization of a magnetohydrodynamic (MHD) power generator using hydrogen as a fuel has been considered by a number of authors (references 1-9) as a means of producing electrical power. In references 1 and 2 the feasibility of using hydrogen transmitted by pipe from a remote coal gasifier into the city and converted to electricity in a steam MHD plant having an integral gasous oxygen plant was investigated. These steam MHD systems were shown on a performance and cost basis to offer an attractive alternative to both in-city clean fueled conventional steam power plants and to remote coal-fired power plants with underground electric transmission into the city. In references 3-9 the production of hydrogen and oxygen utilizing a nuclear reactor was investigated as a means of load-leveling for the nuclear reactor which due to its high capital cost and operating characteristics should be operated at constant power. The concept studied was to produce H_2-O_2 during off-peak load periods and store them for use in a steam MHD plant during peak load periods. References 3-7 considered hydrogen-oxygen production by electrolysis

while references 8 and 9 considered thermochemical decomposition of water. All of the above studies were conceptual systems studies. In the present paper we will discuss our experimental investigation of the MHD power generation portion of the steam MHD plant.

The Lewis Research Center (LeRC) has in operation a small (4-12 MW_t) cesium-seeded H_2-O_2 combustion MHD generator to investigate performance and fluid dynamics at high magnetic field levels. The MHD power generation experiments are conducted in a high magnetic field strength cryomagnet facility. While this facility has the capability to produce fields 6 tesla, the peak field utilized to date is 5 tesla. In the initial experiments, the Hall generator configuration was chosen for its simplicity of construction and is designed to operate supersonically (Mach 2 at entrance) over a range of combustion pressures (5-20 atm) and a range of oxygen/fuel weight ratios (4-12). This facility and the associated MHD hardware are discussed in Section II.

In our experiments two conically bored ducts having an overall area ratio of 2.56 and 4 respectively have been tested. The effects of power takeoff location, axial duct location within the magnetic field, generator loading, B-field strength, and interelectrode voltage breakdown were investigatged. The effect upon power output of the power takeoff and duct location within the magnetic field are discussed. Effects of generator loading and B-field strength indicate that the overall internal resistance of the Hall generator only weakly depends upon B-field strength, and the power output is proportional to the square of the B-field. It is further shown that additional power output can be obtained by multiple loading of the duct. Electrode breakdown is found to occur with arc damage to the anode wall. This breakdown occurs at interelectrode voltages in the range of 50 volts/insulator. These results are discussed in Section III.

II. EXPERIMENTAL FACILITY

The MHD power generation experiments are conducted in a high field strength cryomagnet (fig. 1) which was adapted from an existing facility. In its original construction, it consisted of 12 high purity aluminum coils which are pool cooled in a bath of liquid neon. In this configuration, a peak field of 15 tesla was produced. For the present experiments, the center four coils were removed and a 23 cm diameter transverse warm bore tube was inserted to allow the placement of the MHD experiment between the remaining eight coils as shown in the cross section insert in figure 1. In this configuration, a peak field of 6 tesla should be obtainable. The time duration of the experiment is limited by the neon supply which allows on the order of one minute of total operating time followed by an 18-hour reliquefaction period. As a result, the experiments are run in a pulsed mode. The run duration for the data presented here was 5 sec.

In the rocket engine modified for use in this program, the gaseous H_2 is injected uniformally into the combustion chamber through a porous stainless steel injection plate at the rear of the chamber. The gasous O_2 is injected through 36 injection tubes uniformally inserted into the H_2 injection plate. Cesium seed required to produce the high electrical conductivity is injected into the oxygen supply line as a 75 percent solution by weight of CsOH dissolved in water. The combustion chamber and nozzle are water-cooled electrodeposited copper capable of steady-state operation. The length of the chamber and nozzle is 22.86 cm and the i.d. of the chamber is 6.35 cm.

The nozzle is designed for Mach 2 at the 4.96 cm diameter exit. The engine is capable of operation at stagnation pressures between 5 and 20 atm and at O/F weight ratios from 4-12.

Experiments have been carried out using a diverging circular cross section duct having an inlet Mach number 2. Two ducts having exit to inlet area ratios of 2.56 and 4, respectively have been tested. The heat sink duct is constructed from 42 cooper electrodes, 1.27 cm wide and electrically insulated from one another by a high-temperature asbestos sheet (to provide pressure seal), sandwiched between two sheets of mica (to provide electrical insulation). The duct (figure 2) is built up in modular form, each module consisting of 8-15.24 cm o.d. rings clamped together between two triangular shaped pieces by three electrically insulated stainless steel bolts. Lateral movement of the rings is negated by three fiberglas rods inserted through the entire module. Four such modules are used in the present experiments with 2.54 cm end flanges for a total of 42 electrodes. Figure 2 is a picture of the combustor-generator-diffuser assembly.

The entire combustor-generator-diffuser assembly is inserted in the bore tube as shown in figure 1. The high-temperature exhaust gases are water quenched at the exit of the diffuser. The resulting water then passes back to a sump for recirculation. The water is periodically brought back to normal PH by acid addition after which it can be discarded through storm sewers.

While the facility is capable of being run over a wide range of parameters, the data which will be discussed in this report was taken for the following nominal conditions:

Combustion stagnation pressure	10 atm
Mass flow rate	.5 kg/sec
Seed fraction = $\frac{\text{wt. of Cs}}{\text{tot. wt.}}$	.05
Equivalence ratio	1.0
Thermal input	7 MW
Peak magnetic field	5 tesla
Entrance Mach number	2
Duct Entrance diameter	5.0 cm
Duct exit diameter	
2.56 AR duct	8.0 cm
4.00 AR duct	10.0 cm
Length of duct	58 cm

III. EXPERIMENTAL RESULTS

Effect of Power Takeoff and Axial Duct Location

In these initial experiments, the Hall generator configuration was chosen over the more efficient Faraday or diagonal wall (DW) configurations due to its simplicity of construction. One advantage of the Hall and DW configurations over that of the Faraday is that power can be extracted by a single electrical load rather than requiring separate loads for each electrode. However, to obtain maximum power output the internal generator resistance must equal the load resistance. Since as the gas properties (particularly the electrical conductivity) change down the channel, the axially varying local internal impedance cannot be matched by the single external impedance at every point. This is a particularly important point for the H_2-O_2 MHD topping plant

since the pressure ratio through the duct varies by a factor of 100 or more (references 1-9). This is in comparison to present MHD generator experience in fossil fueled systems oxidized by air where the pressure ratios are of order 5.

The result of this effect is shown in figure 3 for the 2.56 AR duct. In this figure the generated voltage is plotted as a function of distance down the channel, i.e., electrode number. In Run 407, the external load (11.5Ω) was placed between the first three and the last three electrodes. It is seen that the voltage gradient between the third and twelfth electrode is negative indicating that power is being dissipated in this region. This is due to the fact that insufficient voltage is being generated in this region to pass the current generated by the generator as a whole.

By eliminating this region from the load, i.e., moving the front power takeoff from electrodes 1-3 to electrodes 10-16, the power output was increased from 8.74 KW in Run 407 to 11.2 KW in Run 413. In the experimental data to be discussed for the 2.56 AR duct, the power takeoff electrodes were 11-13 and 40-42. It should also be noted from figure 3, that in Run 413 the voltage gradient between electrodes 1-10 is now positive, and hence additional power could be obtained from this region by loading it with an appropriately matched impedance. The effect of multiple loading will be discussed in the next section.

When the 4 AR duct was loaded from the first three to the last three electrodes the region of negative power generation moved downstream to approximately the 15th electrode as compared to the 12th electrode as observed in the 2.56 AR duct. This resulted from the increased overall performance of the 4 AR duct and the fact that the increased area ratio was achieved by conically boring the duct from a fixed inlet area. Therefore increased performance was achieved in the downstream portion of the channel with little performance change upstream. As a result a greater portion of the upstream region of the duct was unable to support the increased performance of the duct as a whole so that maximum power output is achieved by excluding this region from the load. Unless otherwise noted the experimental data to be discussed for the 4 AR duct was obtained with the power takeoff electrodes connected from 14-16 to 40-42.

Also to be noted from figure 3 (for 2.56 AR duct) and figure 4 - Run 708 (for 4 AR duct) is that the generated voltage at the end of the duct is still rising on a positive slope. This indicates that the magnetic field is still of sufficient strength beyond the end of the duct to allow additional power production. In order to investigate this possibility, tests were run with the 4/1 area ratio duct moved downstream relative to the centerline of the magnet. The results are shown in figure 4. In this figure the magnetic field profile is shown in relation to the various duct locations. The axial voltage profiles as a function of distance from the magnet centerline are shown for the duct load resistance connected from electrodes 1-3 to 40-42. The curve labeled Run 708 was the location of both the 2.56 AR and the 4 AR ducts during the tests discussed throughout the rest of the paper. Figure 4 shows that the effect of moving the duct downstream is to decrease the region of negative power generation in the front of the duct (Run 1012). However, as the duct is moved further downstream (Run 1006) the magnetic field at the end of the generator finally becomes too small to generate sufficient voltage to maintain the current generated by the duct as a whole. As a result a region of negative power generation is produced at the end of the duct which decreases the power output. Therefore there is an optimal location for the present duct

within the magnetic field which is approximately that of Run 1012.

As a result of the loading and duct location tests discussed in this section, it can be concluded that a more optimal utilization of the magnetic field could be obtained with a longer duct. This would allow the use of the full extent of the downstream magnetic field while the upstream region of negative power generation could be made power producing by separately loading the front and rear regions of the duct with a common junction point at the inflection point of the voltage versus distance curve as discussed in the next section.

Effect of External Loading and B-Field

Figure 5 shows the loading diagram for the 2.56/1 area ratio duct at various magnetic field strengths. The scatter in the data is shown by the error bars about the circled point which is the average. The surprising result of this plot is that the internal impedance (as measured by the slope of the curves) is relatively independant of the magnetic field. The internal impedance as measured in this manner is plotted in Figure 6 as a function of magnetic field strength. It is seen that the dependence is weak which is not what one would expect from the theoretical relation for a Hall generator

$$R = \int_0^{\ell} \frac{1 + \beta^2}{\sigma A} \, dx$$

where R is the internal impedance, ℓ is the length of the power generating region, β is the Hall parameter, σ is the electrical conductivity, and A is the duct cross sectional area.

For the conditions of the present experiments, β is in the range of 1-2 and hence one would expect that R would be sensitive to the magnetic field strength. However, theoretical calculations indicate that the $\underline{j} \times \underline{B}$ force is of sufficient magnitude so as to slow the plasma down to a degree that causes the temperature to increase in the power generation region. This results in an increase in σ which compensates to a large degree for the increase in $1 + \beta^2$.

Similar results, although not in as great a detail, were found for the 4/1 area ratio duct. Also during the test of this duct the question of multiple loading was investigated. Although maximum power with a single load is extracted from the region of electrodes 14-16 to 40-42, the upstream region in this configuration (electrodes 1-14) generates a positive open circuit voltage (as in the 2.56 AR duct, see Run 413 of figure 2) and hence could be used to generate power by separately loading this region. It was therefore of interest to see if indeed additional power could be generated in this manner and also to see if this affected the power production in the downstream region.

In figure 7 the output voltage for the 4 AR duct is shown as a function of electrode number for the optimum configuration for the multiple load case. In this case electrodes 6-15 were connected through a 10 Ω load while electrodes 15-42 were connected through a 12 Ω load. As in the single load case in which the load was across the entire duct, a region of negative power generation was found to exist in the region from electrodes 1-6 when the front end load was connected from electrodes 1-15. Therefore maximum power was obtained by excluding this region from the load. However, as can be seen from figure 7, the region possesses a positive open circuit voltage and

additional power could be extracted by separately loading this region.

In the case of our small experiment, properties do not change greatly over the power generation region and hence the majority of the power (95%)can be extracted from a single load. However, in the actual H_2-O_2 MHD topping plant large pressure ratios (~ 100) and large extractions of the input enthalpy (~40%) will result in significant variations in working fluid properties, and optimal performance will require multiple loading.

Power Output

In figure 8, the effect of B-field on the power generated for a single load is shown for the 2.56 AR and 4 AR ducts operating at a combustion pressure of 10 atm. It is seen that for the operating conditions and geometry of the present experiments that the power increases linearly with B^2. However, the theoretical dependence of power upon B-field is a complicated function of several factors so that it can not be concluded that this dependence will in general apply to all operating conditions or duct geometries. One complicting factor is discussed in the next paragraph. The maximum power output achieved for the 2.56 AR and 4 AR ducts was 87.5 KW and 153 KW, respectively.

Tests in the 2.56 AR duct were carried out over a pressure range of 5 to 13 atm. While the testing was not extensive at other than 10 atm, no shocks or flow separations were observed within the duct. In the 4 AR duct a shock was observed in the duct even without power extraction for pressures at and below approximately 7 atm. The influence of B-field (power extraction) upon the location of the shock within the duct is shown in figure 9. It is seen that the shock moves upstream with increased B-field (power extraction). This has a profound influence upon the power that can be extracted from the channel, since in the region downstream of the shock the flow is subsonic and the reduced velocity results in a decrease in generated voltage. This is shown in figure 10 where the power output is plotted versus the square of the B-field. It is seen that while the power output still increases with B-field the previously observed linear dependence at a combustion pressure of 10 atm no longer exists at a combustion pressure of 7 atm, and that the rate of power increase falls rapidly with increased B-field. The question of shock formation and/or flow separation is of particular importance in the H_2-O_2 MHD topping plant due to the large (~ 40%) enthalpy extractions which are required. This will require energy to be extracted not only from the enthalpy of the working fluid but also from its kinetic energy. This conversion of kinetic energy into power results in the slowing down of the gas with the attendant problem of producing adverse pressure gradients which can result in flow separation such as noted in subsonic diffusers.

In figure 11 the power density as a function of distance down the channel is plotted for the 2.56 AR and 4 AR ducts at a B-field strength of 5 tesla and a combustion pressure of 10 atm. These curves were obtained by differentiating the measured Hall votage profiles to obtain the local Hall electric field and by assuming that the measured Hall current completely and uniformly fills the duct cross sectional area so that the local current density can be obtained by dividing the measured current by the area. As can be seen from figure 11 the peak power density is substantially increased in the 4 AR duct as compared to the 2.56 AR duct being 110 MW/M^3 and 85 MW/M^3 respectively.

Voltage Breakdown

In the H_2-O_2 MHD topping plant the problem of Hall (axial electric field) breakdown across insulator gaps poses a serious problem due to the low pressures (~.1 atm) at the downstream end of the duct. Since the Hall electric field is proportional to the Hall parameter which is inversely proportional to the pressure, large Hall electric fields will be generated in this region. Therefore the question of breakdown is of key significance in these devices. In the above experiments, no electrical breakdown was observed. However, the interelectrode stress did not not exceed the normally accepted breakdown level of ~40 volts/insulator. In order to determine if the H_2-O_2 combustion system would be limited by the same breakdown level, the generator was operated open circuit. In figure 12 the open circuit Hall voltage for the 2.56 AR duct is plotted versus the square of the magnetic field. During the duration of our 5 second runs, no breakdown is observed below an average field of approximately 50 volts/insulator. Above this value the voltage still continues to increase with B^2. However, approximately 2.5 seconds after initiation of seed injection, breakdown occurs. After breakdown, steady average voltage of approximately 40 volts/insulator is observed independent of magnetic field strength.

Upon disassembly of the channel, grooves approximately one-sixteenth of an inch wide perpendicular to the magnetic field were found to exist on the interelectrode insulators on the anode side of the channel. The damage was typical of the insulator shown in the upper right-hand corner of figure 13. The severity of the damage to the insulators (as measured by the length of the grooves) very nearly correlated to the power density profile shown in figure 11. This effect was also observed in references 10 and 11. The $\underline{j} \times \underline{B}$ force acting on the shorted current forces it into the insulators on the anode side of the channel resulting in the grooves. On the cathode side of the channel the $\underline{j} \times \underline{B}$ force drives the shorted current away from the insulators.

At this point, the duct had approximately 20 minutes of test time on it. In order to determine if the observed insulator damage was due solely to breakdown or just to general deterioration, the channel was rebuilt with new insulators. In the next series of tests, the duct was operated in the breakdown region with breakdown being observed on approximately one-third of the test runs. After approximately 2.4 minutes of test time, $CsOH/H_2O$ leakage was observed through an electrode insulator and the experiment was stopped. Inspection of the insulators showed the severe damage as shown by the other three insulators in figure 13. The channel was again rebuilt and operated below the breakdown region for an accumulative run time of 5.5 minutes with no observable damage to the insulators indicating that insulator damage was solely due to arc breakdown at the anodes.

CONCLUDING REMARKS

While the results achieved in the present experiments are encouraging from the standpoint of realizing the utilization of H_2-O_2 MHD/steam power plants, there are still significant questions to be answered. These include:

1. Whether the large enthalpy extractions (~40%) required in the H_2-O_2 MHD topping plant to make these plants attractive can be achieved in actual practice. In MHD power generating systems utilizing fossil fuels oxidized by high temperature and/or oxygen enriched air enthalpy extractions of 20% lead to acceptable system

efficiencies. However, even with the enormous research effort being expended in this area demonstration of this much lower enthalpy extraction is yet to be achieved.

2. The experiments discussed in this paper were limited to exhausting the working fluid at atmospheric pressure. In the actual H_2-O_2 MHD topping plant the exhaust is to very low subatmospheric pressures. The performance of the MHD generator at these low pressure is yet to be established.

These questions will not be answered in our present test facility. The demonstration of large enthalpy extraction requires large scale facilities in which the wall dominating losses due to friction, heat transfer, and voltage drops become neglible as compared to the volume production of MHD electric power. The demonstration of MHD generator performance at the low subatmospheric pressures of H_2-O_2 MHD power plant obviously requires a vaccum system which is not available in the present facility.

In experiments now in progress, a duct approximately 25% longer (to better utilize the available magnetic) with electrode rings .64 cm thick as compared to the 1.27 cm thickness of our present duct (to increase the breakdown voltage) is being tested at area ratios greater than 4.

REFERENCES

1. Seikel, G. R., Smith, J. M., Nichols, L.D. (1974) H_2-O_2 Combustion Powered Steam-MHD Central Power Systems. In T. N. Veziroglu (Ed.), Hydrogen Energy, Part, B, Plenum Press, New York, pp. 969-982.

2. Smith, J. M., Nichols, L. D., Seikel, G. R. (1974) NASA Lewis H_2-O_2 MHD Program. In 14th Symposium Engineering Aspects of Magnetohydrodynamics, April 8-10, 1974, The University of Tennessee Space Institute, Tullahoma, Tennessee, pp. III.7.1-5.

3. Townsend, S. J., and Koziak, W. W. (1974) The Use of Hydrogen/Oxygen/Cesium Hydroxide MHD Generation/Steam Turbine Combustion for Storage of Nuclear Energy. Paper presented at The Hydrogen Economy Miami Energy (THEME) Conference, March 1974, Miami Beach, Florida (late paper not published in Proceedings).

4. Townsend, S. J., and Koziak, W. W. (1974) An MHD Energy Storage System Comprising a Heavy-Water Producing Electrolysis Plant and a H_2-O_2/CSOH MHD Generator/Steam Turbine Combination to Provide a Means of Transferring Nuclear Reactor Energy from the Base-Load Regime into the Intermediate-Load and Peaking Regimes. In T. N. Veziroglu (Ed.), Hydrogen Energy, Part B, Plenum Press, New York, pp. 983-989.

5. Stangeby, P. C. Potential Applications of MHD Power Generation in Canada. Paper presented at the 14th Symposium, Engineering Aspects of Magnetohydrodynamics, April 8-10, 1974, The University of Tennessee Space Institute, Tullahoma, Tennessee (late paper not published in Proceedings).

6. Stangeby, P. C. (1975) Comparative Economics for H_2-O_2 MHD Emergency and Peaking Power Production. In J. E. Klepeis (Ed.), Sixth International Conference on Magnetohydrodynamic Electrical Power Generation, June 1975, Washington, D. C., Vol. IV, CONF-750601-P4, pp. 9-21.

7. Townsend, S. J. (1975) The Economic Implications of the CANHO H_2-O_2 MHD Energy Storage System Used as an Intermediate-Load and a Peaking Generator. In J. E. Klepeis (Ed.), Sixth International Conference on Magnetohydrodynamic Electrical Power Generation, June 1975, Washington, DC, Vol. V, CONF-75061-P5, pp. 169-176.

8. Nakamura, T., and Riedmuller, W. (1974) Hydrogen-Oxygen Closed Cycle MHD Power Generation System Based Upon Thermochemical Decomposition of Water. In 14th Symposium Engineering Aspects of Magnetohydrodynamics, April 8-10, 1974, The University of Tennessee Space Insitute, Tullahoma, Tennessee, pp. III 6.1-7.

9. Nakamura, T. (1975) Feasibility of Hydrogen-Oxygen Closed Cycle MHD Power Generation Based Upon Thermochemical Decomposition of Water. In J. E. Klepeis (Ed.), Sixth International Conference on Magnetohydrodynamic Electrical Power Generation, June 1975, Washington, D. C., Vol. IV., CONF-750601-P4, pp. 39-52.

10. Zankl, G., Raeder, J., Dorn, C., and Volk, R. (1973) Experimental Determination of Design Data for an MHD Generator. In 13th Symposium, Engineering Aspects of Magnetohydrodynamics, Stanford University, Stanford, California, 1973, pp. II.6.1-7.

11. Beaton, M. S., Scott, M. H., Wu, Y. C. L., Dicks, J. B., Jr., Muehlhauser, J. W., Holt, W. L., and James, H. D. (1978) Insulator Performance and Anode Recession Rate in a Direct Coal Fired Cold Copper Diagonal Conducting Wall MHD Generator. In C. H. Kruger (Ed.), 17th Symposium, Engineering Aspects of Magnetohydrodynamics, 17th, Stanford University, Stanford, California, 1978, pp. D-2.1-D.2.6.

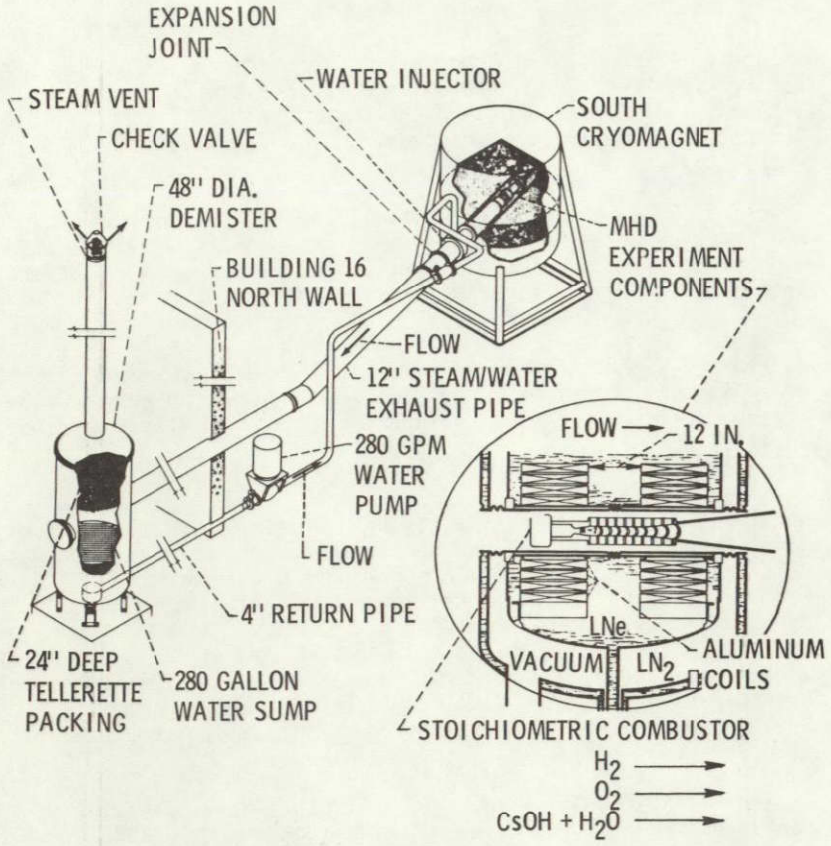

Figure 1. - GH_2-GO_2 combustion MHD experiment installation.

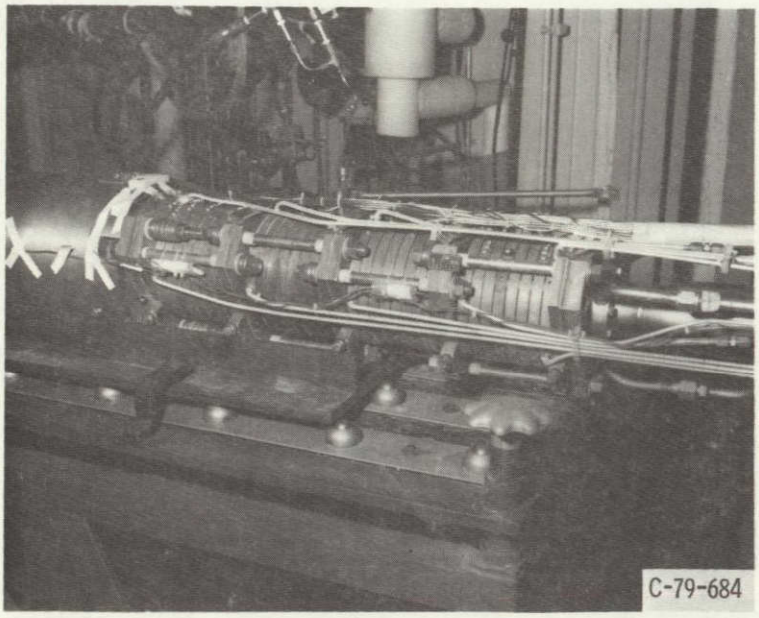

Figure 2. - Combustor-generator-diffuser assembly.

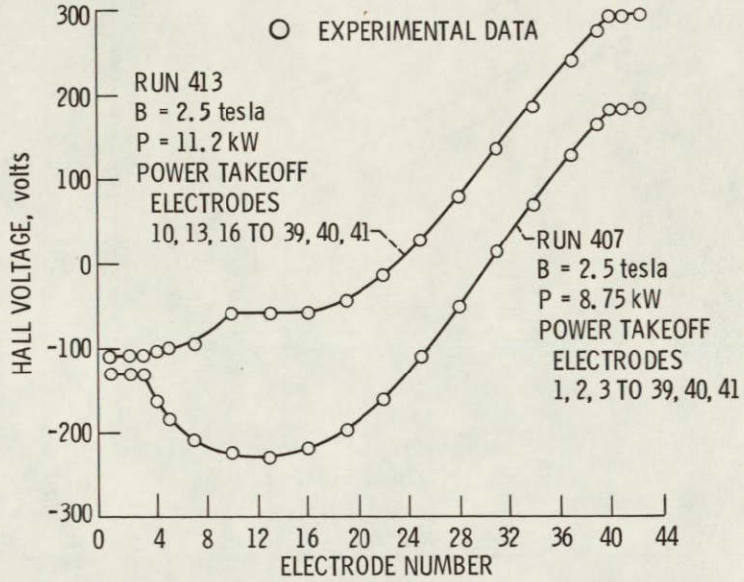

Figure 3. - Effect of electrical load on generator performance (2.56 AR duct).

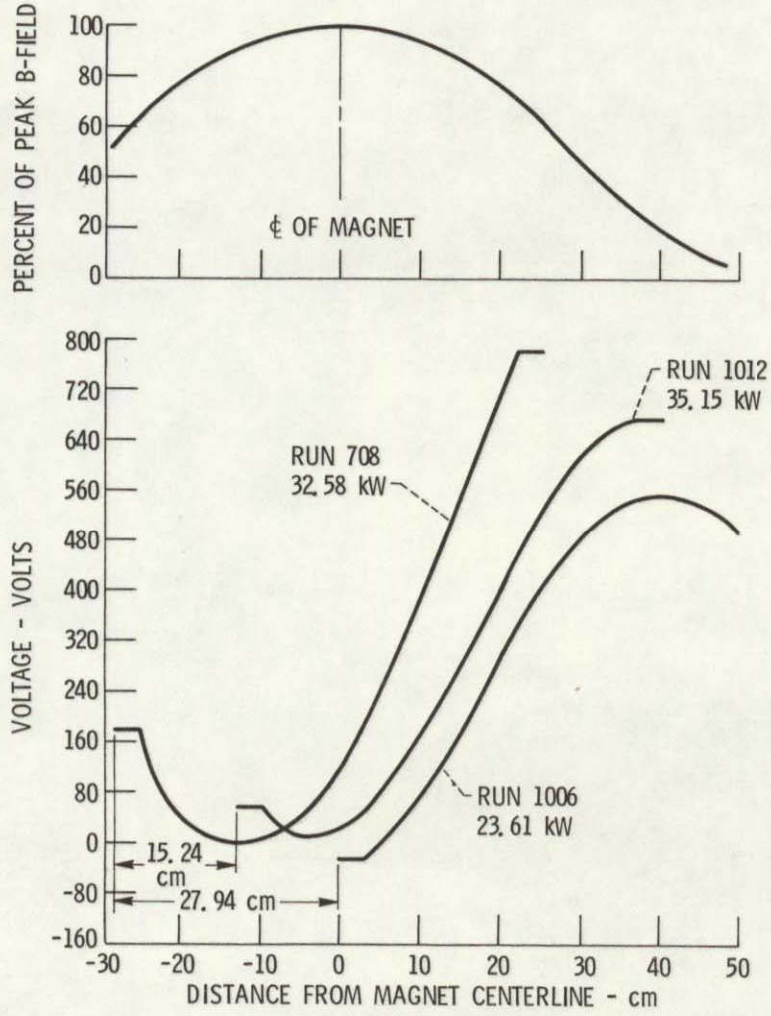

Figure 4. - Magnet field and voltage distribution in 4 to 1 area ratio duct.

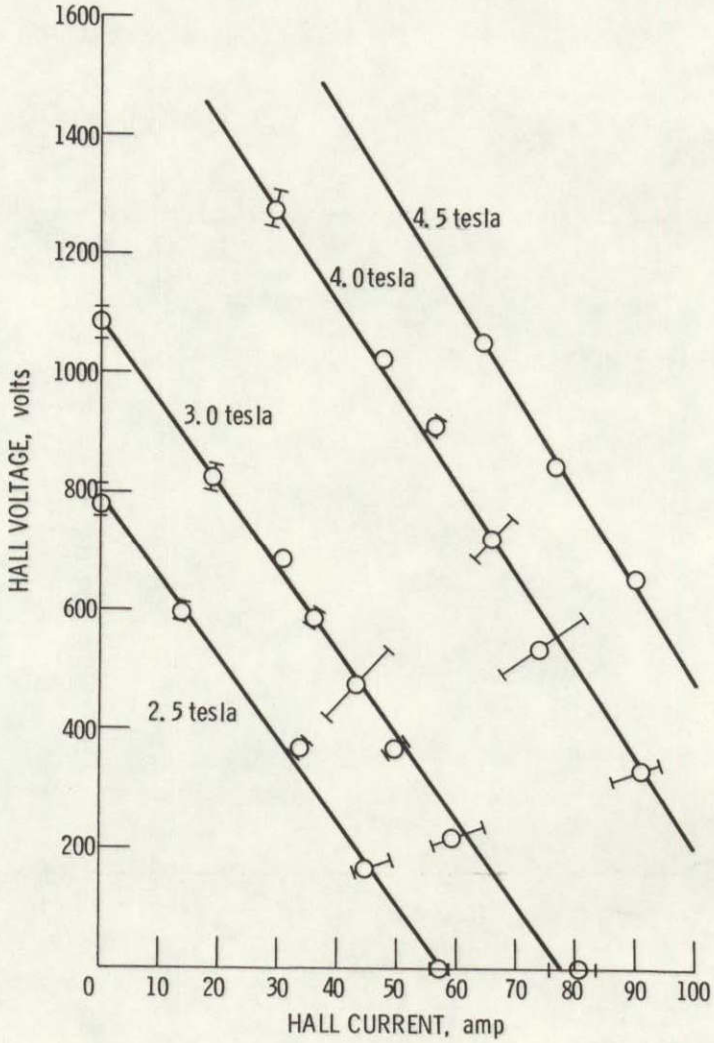

Figure 5. - MHD generator load curve. Power takeoff electrodes 11-13 to 40-42 (2.56 AR duct).

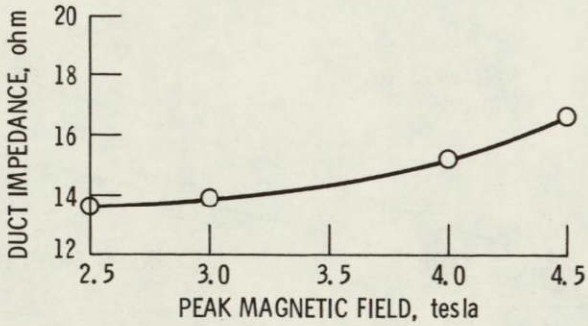

Figure 6. - Duct impedance as function of magnetic field strength (2.56 AR duct).

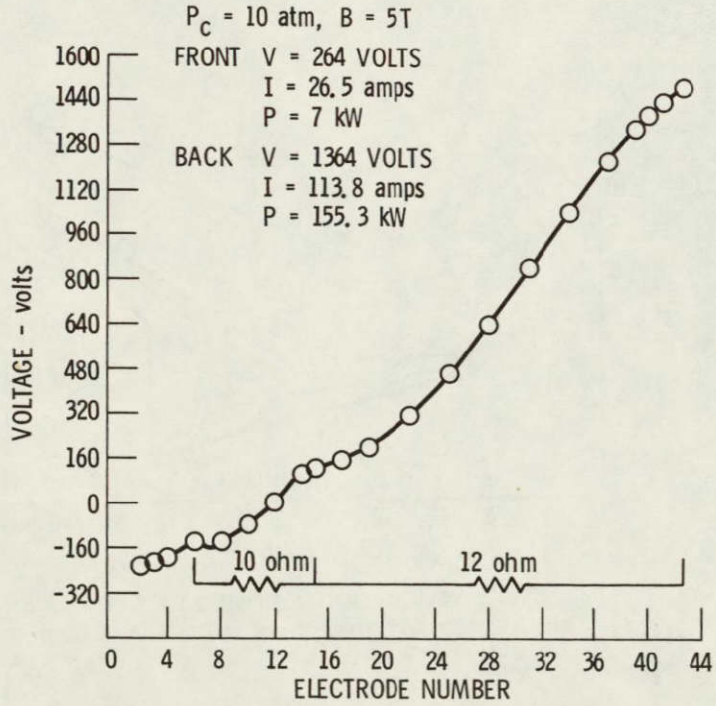

Figure 7. - Axial voltage profile for multiple loading (4 AR duct).

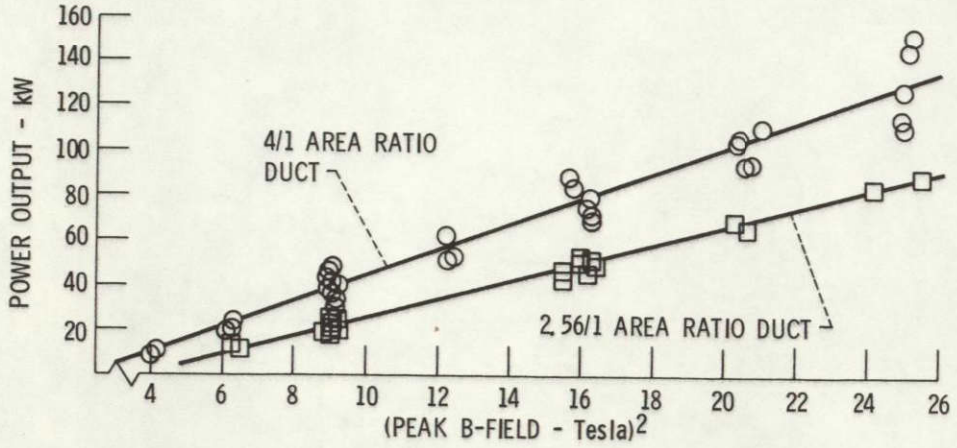

Figure 8. - Power output versus B^2 at P_c = 150 psia.

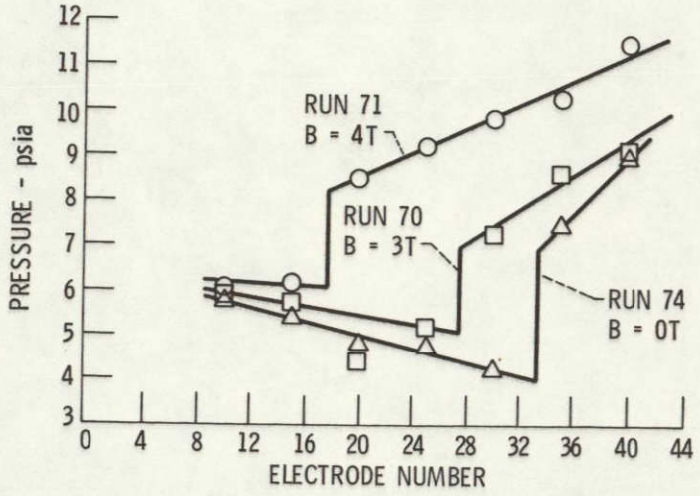

Figure 9. - Axial pressure distribution for various B-fields, combustion pressure of 100 psia (4 AR duct).

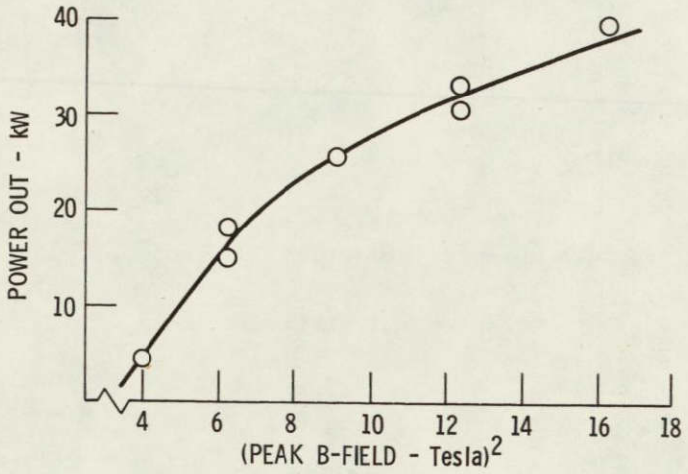

Figure 10. - Power output versus B^2 at P_c = 100 psia (4 AR duct).

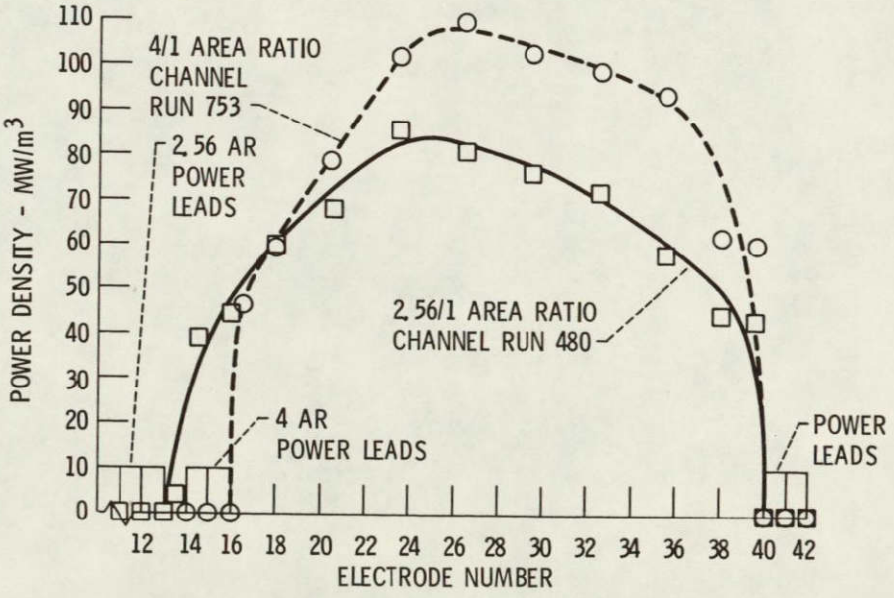

Figure 11. - Power density along channel - B = 5 Tesla, P_c = 10 atm.

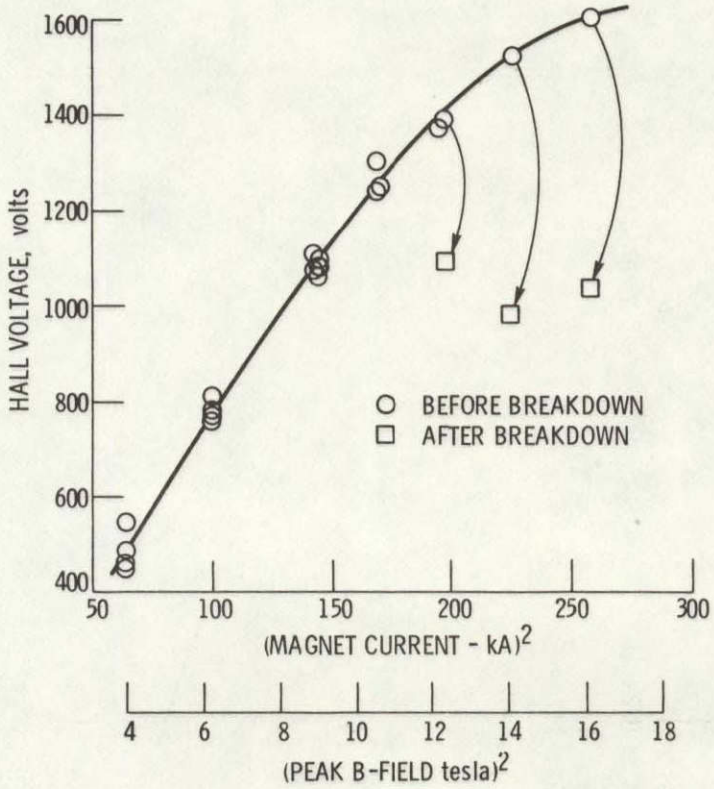

Figure 12. - Hall voltage before and after breakdown (2.56 AR duct).

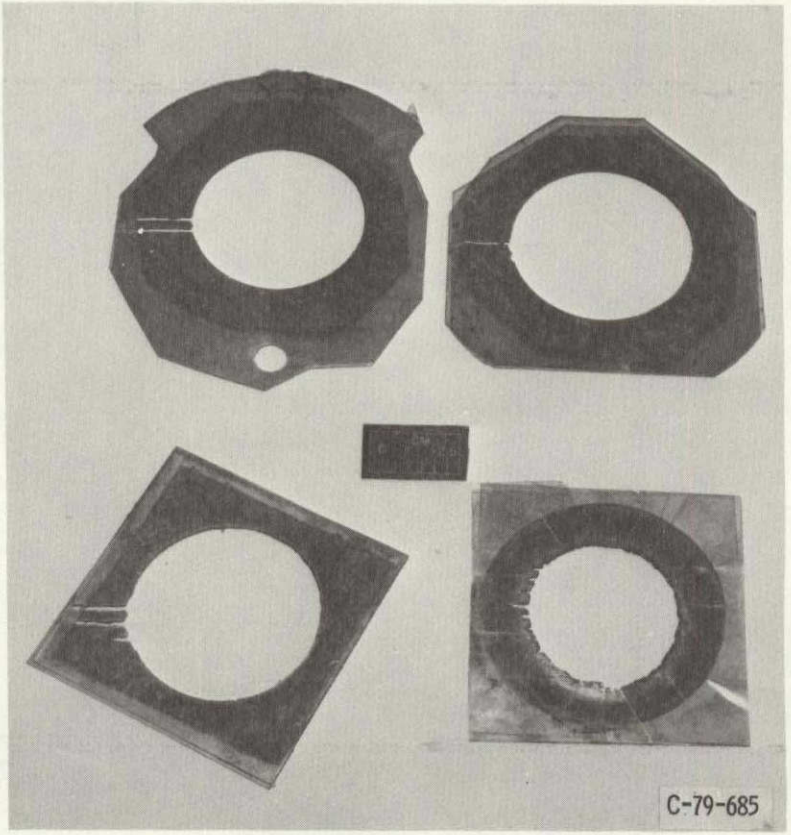

Figure 13. - Interelectrode insulator damage.

1. Report No NASA TM-81424	2 Government Accession No.	3. Recipient's Catalog No.
4. Title and Subtitle EXPERIMENTS ON H_2-O_2 MHD POWER GENERATION		5. Report Date 6. Performing Organization Code
7. Author(s) J. Marlin Smith		8. Performing Organization Report No. E-348 10. Work Unit No.
9. Performing Organization Name and Address National Aeronautics and Space Administration Lewis Research Center Cleveland, Ohio 44135		11. Contract or Grant No. 13. Type of Report and Period Covered Technical Memorandum
12. Sponsoring Agency Name and Address National Aeronautics and Space Administration Washington, D.C. 20546		14. Sponsoring Agency Code
15 Supplementary Notes		

16. Abstract

MHD power generation experiments utilizing a cesium-seeded H_2-O_2 working fluid have been carried out using a diverging area Hall duct having an entrance Mach number of 2. The experiments are conducted in a high-field strength cryomagnet facility at field strengths up to 5 tesla. The effects of power takeoff location, axial duct location within the magnetic field, generator loading, B-field strength, and electrode breakdown voltage were investigated. For the operating conditions of these experiments it is found that the power output increases with the square of the B-field and can be limited by choking of the channel or interelectrode voltage breakdown which occurs at Hall fields greater than 50 volts/insulator. Peak power densities of greater than 100 MW/M^3 have been achieved.

17. Key Words (Suggested by Author(s))	18. Distribution Statement
Magnetohydrodynamics; Power generation; H_2-O_2 combustion; Hydrogen economy; Cryomagnet	Unclassified - unlimited STAR Category 75

19. Security Classif. (of this report)	20. Security Classif. (of this page)	21 No of Pages	22 Price*
Unclassified	Unclassified		

* For sale by the National Technical Information Service, Springfield, Virginia 22161

National Aeronautics and Space Administration

Washington, D.C.
20546

Official Business
Penalty for Private Use, $300

SPECIAL FOURTH CLASS MAIL
BOOK

Postage and Fees Paid
National Aeronautics and
Space Administration
NASA-451

POSTMASTER: If Undeliverable (Section 158 Postal Manual) Do Not Return